LBNL-40219

Energy loss effects on charm and bottom production in high-energy heavy-ion collisions

Ziwei Lin[a], Ramona Vogt[a,b] and Xin-Nian Wang[a]

[a]Nuclear Science Division, LBNL, Berkeley, CA 94720

[b]Physics Department, University of California at Davis, Davis, CA 95616

Abstract

We study the effect of energy loss on charm and bottom quarks in high-energy heavy-ion collisions including longitudinal expansion and partial thermalization. We find that high $p_\perp$ heavy quarks are greatly suppressed, and consequently, high-mass dileptons from heavy quark decays are also suppressed. We consider in detail the detector geometry and single lepton energy cuts of the PHENIX detector at the Relativistic Heavy Ion Collider (RHIC). Because of the longitudinal expansion, the suppressions of $ee, e\mu$ and $\mu\mu$ pairs resulting from the heavy quark energy loss are very different due to the different rapidity coverages and energy cuts. The assumed energy loss rate, on the order of 1 GeV/fm, results in a large suppression on dielectrons, and dielectrons from heavy quark decays become comparable or even lower than the Drell-Yan yield. It is thus possible to probe the energy loss rate of the medium using dileptons from heavy quark decays.

I. INTRODUCTION

A dense parton system is expected to be formed in the early stage of relativistic heavy-ion collisions at RHIC energies and above, due to the onset of hard and semi-hard parton scatterings. Interactions among the produced partons in this dense medium will most likely lead to partial thermalization and formation of a quark-gluon plasma. It is thus important to study phenomenological signals of the early parton dynamics, a crucial step towards establishing evidence for a strongly *interacting* initial system and its approach to thermal equilibrium. Jet quenching is a very good candidate for such a signal since a fast parton traversing dense matter must experience multiple scatterings and suffer radiative energy loss [1–3]. Taking into account multiple scatterings and the so-called Landau-Pomeranchuk-Midgal effect, the energy loss of a fast quark, $-dE/dx \simeq 3\alpha_s < p_{\perp w}^2 > /8$ [3], is found to be completely controlled by the the characteristic broadening of the transverse momentum squared of the fast parton, $< p_{\perp w}^2 >$, which in turn is determined by the properties of the medium. Therefore the energy loss of fast partons is a good probe of dense matter [4].

In principle, the energy loss by a parton in medium, both by radiative [1–3] and elastic [5,6] processes, is independent of the quark mass in the infinite energy limit. At finite energies, studies show that the elastic energy loss has a weak mass dependence. For example, at 10 GeV with α_s=0.2, $n_f = 2$ and a temperature of 250 MeV, the elastic dE/dx for a massless quark and a charm quark is about -0.25 and -0.22 GeV/fm, respectively. We expect that the situation for radiative energy loss is similar, though a detailed analysis is beyond the scope of this paper. Instead, we study the phenomenological consequences of heavy quark energy loss with several values of dE/dx (-2, -1 and -0.5 GeV/fm).

Since parton energy loss results in the suppression of leading particle productions from the corresponding jet, the particle spectra in central $A + A$ collisions and their modification from pp collisions, either in normal events [4] or photon-jet events [7], can be used to study the parton energy loss. For this reason, energetic charm and bottom mesons are particularly good leading particles because they carry most of the charm or bottom quark's energy. The

energy loss of fast charm or bottom quarks will be directly reflected in the suppression of large p_T charm or bottom mesons.

Unfortunately, it is difficult to detect charm or bottom mesons directly with current tracking technology because of the large number of produced particles in central $A + A$ collisions at RHIC. However, it was pointed out in earlier studies [8–10] that leptons from the decay of charm mesons will dominate the dilepton spectrum over that from bottom decays and the Drell-Yan process in the large invariant mass region beyond the J/ψ. Since the invariant mass of the lepton pairs from charm decays is related to the relative momentum of the $D\bar{D}$ pair, the dilepton yields in this region could become an indirect measurement of the charm spectrum. Therefore, it should be sensitive to the energy loss suffered by the charm quarks if they propagate through dense matter. Shuryak [11] recently studied the effect of the energy loss on heavy quarks in $A + A$ collisions and found that heavy quark pairs at large invariant mass are suppressed. Consequently dileptons from their decays are also suppressed. However, this study only considered heavy quarks in the central rapidity region. Moreover, thermal fluctuations are also neglected so that most heavy quarks are at rest, stopped in the dense medium.

In this paper, we re-examine the effects of heavy quark energy loss, including the longitudinal expansion and thermal fluctuations, which are important for the dilepton spectrum from heavy quark decays. Because of the longitudinal expansion, the momentum loss in the longitudinal direction is quite different from that in the transverse direction. The resulting suppression of high invariant mass dileptons from heavy quark decays is then very sensitive to the phase space restrictions imposed by the detector design, *e.g.*, PHENIX at RHIC. Heavy quarks cannot be at rest in a thermal environment. In the most extreme scenario when they are thermalized, they must have a thermal momentum distribution in their local frame. The resulting heavy quark spectrum and the corresponding dilepton spectrum will then be different from that obtained by Shuryak [11]. We use a Poisson distribution for the number of scatterings to model the effects of fluctuations in the number of multiple scatterings in a finite system. In this case, the heavy quarks have a finite probability of escaping

the system without interactions or energy loss.

This paper is organized as follows. We first explain our simple model for energy loss in section II. In section III, we discuss the effect of energy loss on the charm and bottom quark spectra within our model. In section IV, we show the resulting dilepton spectra from correlated heavy quark decays. To demonstrate the sensitivity to the phase space restriction, in section V we calculate the spectra of $e^+e^-, e^\pm\mu^\mp$ and $\mu^+\mu^-$ pairs from correlated charm decays within the planned acceptance of the PHENIX detector, taking into account the detector geometry and single lepton energy cuts. If high mass dileptons from open charm decays are suppressed by the energy loss, dileptons from bottom decays can become important, especially after imposing the single lepton energy cuts, because these decays can generate more energetic leptons due to the larger bottom quark mass. Therefore we study the energy loss effects on both charm and bottom quarks in this paper. To study the sensitivity to the longitudinal expansion pattern of the dense matter, we compare the results from our model with those from a static fireball model where the longitudinal expansion and the thermal effect are neglected so that the heavy quarks energy loss is isotropic. The energy loss rate, dE/dx, is -2 GeV/fm if not specified otherwise. We also study the sensitivity of single lepton and dilepton production to the magnitude of the energy loss by comparing results with different values of dE/dx. In section VI we calculate the single e and μ spectra from charm and bottom decays within the PHENIX acceptance. We summarize in section VII.

II. THE MODEL

In order to implement the energy loss of heavy quarks, we need to specify the phase space distribution of the heavy quarks and the space-time evolution of the dense matter. For heavy-ion collisions at collider energies, we use the Bjorken model [12] to evolve the system. The dense matter then has a fluid velocity $v_z^F = z/t$ in the longitudinal direction. This is essentially the fluid velocity of free-streaming particles produced at $z = 0$ and

$t = 0$. We neglect the transverse flow which sets in at a much later time. We also neglect the formation times of both the heavy quarks and the dense medium. Therefore heavy quarks are produced at $z = 0$, the same point at which the expansion begins. Then, for any given space-time point, (z, t), a heavy quark will find itself in a fluid with the same longitudinal velocity. Therefore in the fluid rest frame, the heavy quark has momentum $(0, \vec{p}_\perp)$. Energy loss reduces the heavy quark momentum to $(0, \vec{p_\perp}')$ in the fluid rest frame so that the momentum of the heavy quark changes from $(m_\perp \sinh y, \vec{p}_\perp)$ to $(m'_\perp \sinh y, \vec{p_\perp}')$ in the lab frame. Thus a heavy quark loses its transverse momentum but retains its rapidity because it follows the longitudinal flow. We will only consider fluctuations in the longitudinal momentum when a quark loses most of its energy as we shall describe below.

Since we neglect the transverse expansion, the transverse area is the area of the nucleus. The probability of heavy quark production as a function of the transverse radius is proportional to the overlap function of the two nuclei at zero impact parameter. To simplify the calculations, we assume spherical nuclei of radius $r_A = r_0 A^{1/3}$. Since the heavy quarks have a finite probability to escape without interaction or energy loss, we introduce the mean-free-path of the heavy quark in the dense matter, λ, in addition to the average energy loss per unit length, dE/dx. For a heavy quark with a transverse path, $l_\perp$, in the medium, $\mu = l_\perp/\lambda$ gives the average number of scatterings. We then generate the actual number of scatterings, n, from the Poisson distribution, $P(n, \mu) = e^{-\mu}\mu^n/n!$. This corona effect is particularly important for heavy quarks produced at the edge of the transverse plane of the collision. In the rest frame of the medium, the heavy quark then experiences momentum loss $\Delta p = n\lambda \, dE/dx$.

When a heavy quark loses most of its momentum in the fluid rest frame, it begins to thermalize with the dense medium. To include this thermal effect, we consider the heavy quark to be thermalized if its final transverse momentum after energy loss, $p'_\perp$, is smaller than the average transverse momentum of thermalized heavy quarks with a temperature T. These thermalized heavy quarks are then given a random thermal momentum in the rest frame of the fluid generated from the thermal distribution $dN/d^3p \propto \exp(-E/T)$. The

final momentum of the thermalized heavy quark is obtained by transforming back from the local fluid frame with a velocity of z/t to the center-of-mass frame of the collision. In our calculations, we assume $\lambda = 1$ fm and $T = 150$ MeV.

III. EFFECTS OF ENERGY LOSS ON HEAVY QUARKS

We generate the momentum distribution of $c\bar{c}$ pairs from the HIJING program [13]. Initial and final state radiation effectively simulates higher-order contributions to charm production so that the pair is no longer azimuthally back-to-back as at leading order. In principle, the momentum distribution of the pair can be calculated at next-to-leading order [14]. In practice, however, next-to-leading order numerical programs [15,16] must cancel singularities in order to obtain a finite result [17]. This is relatively easy if one integrates the cross section over part of the phase space. It is, however, difficult to numerically cancel these divergences when the complete kinematics of the heavy quark pair are desired. Since we would like to use the dilepton spectra from correlated charm decays as an indirect measurement of charm production, it is imperative that we have the complete information of the charm pair, including the momentum correlation between the c and $\overline{c}$.

In the calculation of open charm production with the HIJING program, we use the MRS D$-'$ [18] parton distribution functions with $m_c = 1.3$ GeV. We normalize the calculation so that the charm pair production cross section is 340 μb in $\sqrt{s} = 200$ GeV pp collisions at RHIC. With an $A^{4/3}$ scaling and an inelastic pp cross section of 40 mb, this results in an average of 9.7 charm pairs in a central Au+Au event at RHIC. Shadowing effects on the nuclear parton distribution functions, not large for large invariant mass pairs, are not included.

We now study the effect of energy loss on the charm quark spectra in the simple model we have described. Fig. 1 shows the $p_\perp$ spectrum of charm and anti-charm quarks. It is normalized to one central Au+Au event at RHIC, as are all the other figures. With $dE/dx = -2$ GeV/fm, $\lambda = 1$ fm, and $T = 150$ MeV for thermalized charm, the spectrum

(solid) is softer than the initial distribution (long-dashed). The yield of high $p_\perp$ charm quarks is suppressed by an order of magnitude. High $p_\perp$ charm quarks are mostly those with enough energy to escape the dense matter. After losing much of its momentum, a charm quark will become part of the thermalized system. The $p_\perp$ distribution of these charm quarks is shown as the short-dashed curve in Fig. 1. In the static fireball model, where expansion and thermal effects are neglected, most of the charm quarks are stopped inside the dense matter. Therefore, the spectrum has a peak at zero $p_\perp$. Since the corona effect is also neglected in the fireball model, high-$p_\perp$ charm quarks are suppressed more than in our model. This difference is also reflected in the dilepton spectrum from charm decays.

In Fig. 2 we plot the single charm rapidity distribution with (solid and short-dashed) and without (long-dashed) energy loss. Since charm quarks go with the longitudinal flow in our model, there is little difference between the rapidity spectrum after the energy loss and the initial spectrum. In the static fireball model (short-dashed) however, most charm quarks are stopped at zero rapidity since there is no longitudinal flow. This sensitivity of the charm rapidity distribution to the longitudinal flow pattern can provide information on the expansion of the dense matter. The initial rapidity distribution of charm quarks is not very different from the gluon rapidity distribution. If the initial pressure causes a strong additional longitudinal expansion, the final charm rapidity distribution will probably become broader, similar to other produced particles.

In order to obtain the final D meson distributions, one should convolute the charm quark distribution with a fragmentation function. In hadronic collisions, one can assume a delta-function-like fragmentation function, $\delta(1-z)$, for charm quark fragmentation into D mesons. As a result, the D meson keeps all the momentum of its charm-quark parent [19,20]. Figs. 1 and 2 then also describe the momentum spectrum of D mesons. However, the fragmentation function could be different in a dense medium than in pp collisions. This uncertainty is beyond the scope of this paper.

We also use the HIJING program to calculate $b\bar{b}$ pair production. The bottom pair production cross section with $m_b = 4.75$ GeV is 1.5 μb in $\sqrt{s} = 200$ GeV pp collisions at

RHIC, extrapolating to 0.043 $b\bar{b}$ pairs on average in a central Au+Au event. Although the energy loss experienced by bottom quarks may be different from that of charm quarks, for simplicity we take the same parameters, $dE/dx, \lambda$ and T as for the charm quark energy loss. High $p_\perp$ bottom quarks are suppressed by an order of magnitude, similar to the charm results shown in Fig. 1. We emphasize that the energy loss rate for a heavier quark could be smaller than that for a lighter quark. We will study the sensitivity of our results to the phenomenological dE/dx in section V.

IV. DILEPTONS FROM HEAVY QUARK DECAYS

One can use the dilepton spectrum from charm decays to indirectly measure charm quark production when a direct measurement via tracking is difficult. Measurements of high-mass dileptons are themselves important. Copious thermal dilepton production [21] was proposed as a signal of the formation of a fully thermally and chemically equilibrated quark-gluon plasma. In order to obtain the yields of thermal dileptons, one needs to subtract the background from heavy quark decays. When energy loss was not included, dileptons from open charm decays at RHIC were shown to be about an order of magnitude higher than the contributions from the Drell-Yan process and bottom decays [9,10], making them the dominant background to the proposed thermal dileptons. Energy loss changes the heavy quark momentum distribution as well as the resulting dilepton spectra from heavy quark decays. Therefore, understanding the effect of energy loss on dileptons from heavy quark decays is also an important step towards the observation of thermal dilepton signals.

We computed the dilepton spectra from D meson decays with a Monte Carlo code using JETSET7.4 [22] for D meson decays. The average branching ratios of $\bar{c} \to eX$ and $\bar{c} \to \mu X$ are taken to be 12%. The lepton energy spectrum from D meson semileptonic decays in JETSET7.4 is consistent with the measurement of the MARK-III collaboration [23]. In this paper, only dileptons from correlated charm pair decays are considered, *i.e.*, a single $c\bar{c}$ pair produces the dilepton. The dilepton spectrum from uncorrelated charm pair decays,

higher and softer than that from correlated charm pair decays, may be removed by like-sign subtraction.

The dilepton invariant mass and rapidity are defined as:

$$M_{l^+l^-} = \sqrt{(p^\nu_{l^+} + p^\nu_{l^-})^2}$$
$$Y_{l^+l^-} = \tanh^{-1} \frac{p^z_{l^+} + p^z_{l^-}}{E_{l^+} + E_{l^-}} \ . \quad (1)$$

In Fig. 3, we show the dilepton invariant mass spectrum from correlated charm pair decays without any phase space cuts. Except for the small difference between the electron and muon masses, this spectrum represents both dielectrons and dimuons while the spectrum of opposite-sign $e\mu$ is a factor of two larger. There is a small suppression at large invariant mass in our calculation with energy loss compared to the original spectrum while the yield from the static fireball model is reduced by about two orders of magnitude relative to the original. The two-component nature of the dilepton spectrum from the fireball model can be easily understood. The low-mass peak mainly arises from decays of D mesons at rest in the dense medium while the high-mass tail comes from D mesons energetic enough to escape the system. The dilepton spectrum from the static fireball model and the resultant suppression relative to the original spectrum are very similar to the results from Shuryak's study [11] where only mid-rapidity heavy quarks are considered.

The lepton spectra from bottom decays are also generated from JETSET7.4. We assume b quarks fragment into $B^-, \bar{B}^0, \bar{B}^0_s$ and Λ^0_b with the production fractions of 38%, 38%, 11% and 13%, respectively. Single leptons from bottom decays can be categorized as primary and secondary leptons. Leptons directly produced in the decay ($b \to lX$) are called primary leptons, and those indirectly produced ($b \to cX \to lY$) are called secondary leptons. Primary leptons have a harder energy spectrum than secondary leptons. In the case of decays to e^+ or e^-, a b quark mainly produces primary electrons and secondary positrons although it can also produce a smaller number of primary positrons due to $B^0 - \bar{B}^0$ mixing. The branching ratios of the necessary b quark decays are 9.30% to primary electrons, 2.07% to secondary electrons, 1.25% to primary positrons, and 7.36% to secondary positrons, respectively. The

branching ratios and energy spectra from JETSET7.4, consistent with measurements [25], are almost identical for muons and electrons.

Like dileptons from charm decays, dileptons from bottom decays can come from correlated and uncorrelated decays of bottom pairs. However, uncorrelated pairs from bottom decays are negligible since the average number of bottom quarks per central Au+Au event at RHIC is much less than 1. The total number of dielectrons from a $b\bar{b}$ decay can be readily estimated to be 0.020. Another important source of dileptons from bottom decays is the decay of a single bottom ($b \to cl_1X \to l_1l_2Y$), unlike the case of charm decays. The branching ratio for a b quark to a dielectron is 0.906% from JETSET7.4, therefore this source gives 0.018 dielectrons, comparable to the yield from correlated decays of $b\bar{b}$ pairs and thus must be included.

Fig. 4 shows the invariant mass spectrum of dileptons from bottom decays without any kinematic cuts. The low invariant mass part of the spectrum is dominated by dileptons from single bottom quarks and $b\bar{b}$ pairs with zero relative momentum. The dot-dashed curve comes from single bottom decays and thus does not depend on the energy loss. The suppression of high invariant mass pairs from bottom decays are similar to the charm case shown in Fig. 3. However, the suppression due to the energy loss begins at larger dilepton invariant mass for bottom decays.

Comparing the solid and long-dashed curves in Figs. 3 and 4, one might suppose that the effect of energy loss on dileptons from heavy quark decays is only a factor of 2. However, we must emphasize that this impression is misleading since this spectrum is integrated over all other kinematic variables, including rapidities of the single quarks. In our model, while a heavy quark loses transverse momentum its rapidity is essentially unchanged due to the longitudinal flow. Because of the rapidity gap between the Q and $\bar{Q}$, a heavy quark pair as well as the resulting lepton pair can still have a sizable invariant mass after the energy loss. However, if one selects leptons with a transverse momenta cut, the effect of energy loss becomes much more dramatic, as we will show in the next section where we consider the finite rapidity coverage and single lepton momentum cuts of the PHENIX detector.

V. DILEPTONS FROM HEAVY QUARK DECAYS AS SEEN BY PHENIX

The PHENIX detector at RHIC is designed to measure electromagnetic signals of dense matter. It is therefore well suited to carry out single lepton (e, μ) and dilepton $(ee, e\mu, \mu\mu)$ measurements. In this section we calculate the dilepton yields within the designed PHENIX detector acceptance.

The PHENIX detector [24] has two electron arms and two muon arms. The electron arms cover the central region with electron pseudo-rapidity $-0.35 \leq \eta_e \leq 0.35$, and azimuthal angle $\pm(22.5^\circ \leq \phi_e \leq 112.5^\circ)$. The muon arms cover the forward and backward regions with polar angle $\pm(10^\circ \leq \theta_\mu \leq 35^\circ)$, corresponding to the pseudo-rapidity interval $\pm(1.15 \leq \eta_\mu \leq 2.44)$, along with almost the entire azimuthal angle coverage. We take $E_e > 1$ GeV and $E_\mu > 2$ GeV [24] to reduce the lepton backgrounds from random hadronic decays such as pions.

Fig. 5 shows the invariant mass distribution of three types of dileptons from open charm decays within the acceptance of PHENIX. The $e\mu$ spectrum includes both $e^+\mu^-$ and $e^-\mu^+$. From the comparison of our energy loss results with the initial distributions, we note that the three dilepton yields have strikingly different suppression factors. In the peaks of the spectra, our calculation shows that the ee yield is suppressed roughly by 100, the $e\mu$ yield by 10, and the $\mu\mu$ yield by only 4. The static fireball model, however, gives a suppression of about 3000 for all three dilepton channels.

The large difference between the suppression patterns due to energy loss of the three types of dileptons is a result of our model of the longitudinal flow combined with the PHENIX rapidity coverage and the single lepton energy cut. From the PHENIX detector geometry, the accepted electrons have nearly zero rapidity. Therefore the energy cut of 1 GeV for single electrons is actually a 1 GeV $p_\perp$ cut. However, the accepted muons typically have a rapidity of 2 so that the 2 GeV energy cut corresponds to a $p_\perp$ cut of only 0.5 GeV. As seen in Figs. 1 and 2, in our model of longitudinal flow, energy loss only suppresses high $p_\perp$ charm quarks without strongly affecting the rapidity spectrum. Consequently, high $p_\perp$

leptons from semileptonic charm decays are strongly suppressed while low $p_\perp$ leptons may be slightly enhanced. Therefore the accepted electrons from charm decays in PHENIX are more strongly suppressed than the accepted muons.

To demonstrate the acceptance of the PHENIX detector, in Fig. 6 we show the rapidity distribution of the three types of dileptons from charm quark decays as seen by PHENIX. The ee pairs are centered around $Y_{l^+l^-} \sim 0$, while the $e\mu$ acceptance covers pair rapidity around -1 and 1, and the $\mu\mu$ pairs are found with $Y_{l^+l^-} \sim -2$, 0 and 2. The two-peak nature of the dimuon spectrum in Fig. 5 is a result of the muon rapidity coverage. The low-mass peak comes from two muons in the same arm while the high-mass peak comes from pairs with one muon in each arm. Similarly, the two-peak nature of the dielectron spectrum in Fig. 5 is a result of the two azimuthal electron coverages in PHENIX.

The strong difference in the suppression of the three dilepton spectra from charm quark decay in PHENIX, as seen in Fig. 5, suggests that we should carefully consider how to measure open charm with the PHENIX detector. In a naive scenario, one would expect that the $e\mu$ coincidence measurement can reveal the open charm cross section so that the dielectron and dimuon open charm yields can be extrapolated just by considering the different rapidity coverages. However, energy loss complicates the acceptances for the three dilepton channels from open charm decays, making the proposed extrapolation difficult. As we will see later in this section, this extrapolation becomes even more complicated when bottom decays are included.

The large suppression of dileptons from open charm decays implies that we should also consider dileptons from bottom decays. Due to their larger mass, bottom quarks produce more energetic leptons than do charm quarks, thus dileptons from bottom decays are expected to be less suppressed than those from charm decays and therefore may become important.

Fig. 7 shows the dilepton yields from bottom decays when the PHENIX geometry and energy cuts are applied. Although there is significant suppression due to energy loss at high invariant mass, the peaks of the spectra are not strongly suppressed. In the static fireball

model dielectrons are even enhanced because there are more stopped bottom quarks at zero rapidity and a bottom quark at rest can still produce an electron energetic enough to pass the 1 GeV cut. The dilepton sources from bottom decays in our energy loss model, shown by the solid curves in Fig. 7, are categorized in Fig. 8. Dileptons from single b or $\bar{b}$ decays can only be significant at low invariant mass. At high invariant mass, the dileptons all come from decays of $b\bar{b}$ pairs. Within the PHENIX acceptance, dileptons from bottom pair decays are dominated by dileptons consisting of two primary leptons because primary leptons are more energetic and therefore favored after the energy cuts.

We compare dileptons from bottom decays with those from correlated charm decays in Fig. 9. We also calculate the Drell-Yan yields of dielectrons and dimuons from the HIJING program and plot them in the same figure. Without energy loss, dileptons from charm dominate those from bottom decays as well as the Drell-Yan yield in the invariant mass region below 8 GeV. With an energy loss rate of -2 GeV/fm, dielectrons from $b\bar{b}$ decays dominate those from charm and the Drell-Yan rate dominates both at high invariant mass. This reduction of continuum dileptons from open charm and bottom decays certainly provides a better opportunity to observe possible thermal dileptons from the quark-gluon plasma.

With an energy loss rate of -2 GeV/fm, the $e\mu$ yield is dominated by bottom decays at high invariant mass. The Drell-Yan process does not contribute to the $e\mu$ channel. Thus high-mass $e\mu$ pairs can be used for bottom observation if this energy loss rate will be reached.

The Drell-Yan dimuon yield lies below the second dimuon peak from the suppressed charm quarks at invariant masses above 4 GeV. Moreover, most of the Drell-Yan dimuons are in the same muon arm due to the strong rapidity correlation. The second dimuon peak mainly comes from the pairs with two muons in opposite muon arms. Therefore it is possible to suppress the Drell-Yan dimuons by imposing large-angle cuts and use high-mass dimuons for charm observation, at least in the rapidity region around 0.

To study the sensitivity of the dilepton spectra from heavy quark decays to the energy loss rate, in Fig. 10 we compare calculations with three values of dE/dx, -2 GeV/fm,

-1 GeV/fm, and -0.5 GeV/fm. Within the PHENIX acceptance, high invariant mass dielectrons are the most sensitive to the energy loss. This is expected because high invariant mass dielectrons mainly come from decays of two energetic heavy quarks. As a result of the corona effect, the suppression of high invariant mass dielectrons will saturate at large $-dE/dx$ for a fixed λ. However, low invariant mass dielectrons have a significant contribution from decays of two thermalized heavy quarks. Therefore they are not sensitive to the energy loss and the suppression of low invariant mass dielectrons will saturate at large $-dE/dx$.

With a smaller energy loss rate of -0.5 GeV/fm, dielectron yields from charm and bottom decays are much less suppressed, and become larger than the Drell-Yan yield. This sensitivity of the dielectron yields to the energy loss can be used to probe the property of the dense medium. Dileptons from bottom decays are less sensitive to the energy loss than those from charm decays. As a result, the $e\mu$ yield from bottom decays becomes less dominant relative to that from charm decays when the parameter dE/dx becomes smaller. Since bottom quarks may lose less energy than charm quarks, the $e\mu$ channel may still be dominated by bottom decays and thus provide a measure of bottom production. Dimuons are the least sensitive to the energy loss rate. Dimuons with invariant mass above 4 GeV are dominated by charm decays, and are therefore useful for charm detection.

Energy loss is described by two parameters in our model, dE/dx and λ, where dE/dx describes the average energy loss rate of a fast parton and the mean free path, λ, determines the frequency of scatterings. A larger λ results in a larger probability for the fast parton to escape without energy loss, similar to a smaller dE/dx. This is responsible for the difference in the large-$p_\perp$ suppression between our model and the static fireball model. If we take the limit $\lambda = 0$, the models should agree at large $p_\perp$. One can also probe these two parameters simultaneously as in the study of jet quenching in γ-jet events [7]. However, it is not yet clear how to disentangle these two effects.

VI. SINGLE LEPTONS FROM HEAVY QUARK DECAYS

Single leptons from charm decay have been suggested as an indirect measure of the charm production cross section [26]. This is possible if the background leptons from random decays of hadrons such as pions and kaons can be well understood.

We show the effect of energy loss on single electrons and muons within the PHENIX acceptance in Fig. 11. With energy loss, the electron yield from charm decays is close to that from bottom decays at energies above 2 GeV. Muons from charm decays are less dominant compared to those from bottom decays, though it seems possible to use single muons to measure the open charm cross section. Calculations with three values of dE/dx, -2 GeV/fm, -1 GeV/fm, and -0.5 GeV/fm, are compared in Fig. 12. Single leptons are not as sensitive to the magnitude of dE/dx as the dilepton mass spectra.

Single leptons can be categorized as those from thermalized heavy quarks and those from heavy quarks energetic enough to escape after energy loss. The former mainly reflects the effective thermalization temperature while the latter can provide us with information on the energy loss. Single electrons with energies greater than $2-3$ GeV are mainly from energetic heavy quarks and thus are more sensitive to the energy loss. Muons from energetic heavy quarks start to dominate the spectrum at a higher energy.

VII. SUMMARY AND DISCUSSION

Dileptons from open charm and bottom decays have been calculated for central Au+Au events at RHIC including the effect of energy loss on heavy quarks in dense matter. We assumed a Bjorken-type longitudinal expansion where heavy quarks move with the flow and thus basically do not change their rapidities throughout the evolution of the system. Heavy quarks, however, lose transverse momentum when traveling through the dense matter. Compared to the case without energy loss, heavy quarks at large transverse momentum are greatly suppressed. As a result, dileptons from heavy quark decays are suppressed at high

invariant mass.

With our model of the energy loss, the three types of dileptons ($ee, e\mu, \mu\mu$) from heavy quark decays within the PHENIX acceptance are suppressed very differently because of the energy cuts and the different rapidity coverages. Thus it is difficult to extrapolate the dielectron and dimuon yields from charm decays based on the $e\mu$ coincidence measurement. Within the PHENIX acceptance, dielectrons are the most sensitive to the energy loss, and dielectrons from heavy quark decays become comparable or even lower than the Drell-Yan yield at high invariant mass. Therefore, they are the best observables to study the energy loss if the heavy quark spectrum cannot be measured directly via traditional tracking techniques. Contrary to the case without energy loss, at high invariant mass the $e\mu$ yield may very well be dominated by bottom decays instead of charm decays. In this case, $e\mu$ coincidence in $A+A$ collisions can no longer measure the charm contribution, but could be used for bottom observation. Dimuons above 4 GeV, which are well above the Drell-Yan yield even with a large energy loss rate, can be used for charm observation.

There are a number of uncertainties in our treatment of the energy loss. There are no calculations of the radiative energy loss rate for massive quarks in medium, therefore dE/dx is a parameter in our model. We have neglected the relative formation times. However, the longitudinal velocity of heavy quarks and the dense matter fluid could be mismatched and this will quantitatively affect the results. The rapidity distribution of the final heavy quarks depends sensitively on the flow pattern. If the different suppressions of the three dilepton channels ($ee, e\mu, \mu\mu$) can be established, it will provide important information about the fluid dynamics of the dense medium. We have not considered any change in the energy loss which could be caused by the expansion of the system and the subsequent decrease in the energy density. Transverse flow is not included in our ideal Bjorken picture which could quantitatively change the low $p_\perp$ lepton and low invariant mass dilepton yields in our calculations. However, the qualitative features of our results, such as the suppression of high $p_\perp$ leptons and high invariant mass dileptons as well as the different suppression patterns for the dilepton channels at PHENIX are not likely to change.

To determine whether single leptons or dileptons from heavy quark decays can indeed probe the energy loss, the most important factor is the background from random hadronic decays. Though we have not done an analysis of the hadronic decays in this paper, it needs further study, particularly since high $p_\perp$ pions will also experience quenching effects and therefore be suppressed in high-energy heavy-ion collisions as well.

Acknowledgments: We thank M. Gyulassy for the inspiration and discussions. We thank E. Shuryak for discussions related to his earlier study on this subject. We also thank T. LeCompte and W. Zajc for helpful discussions.

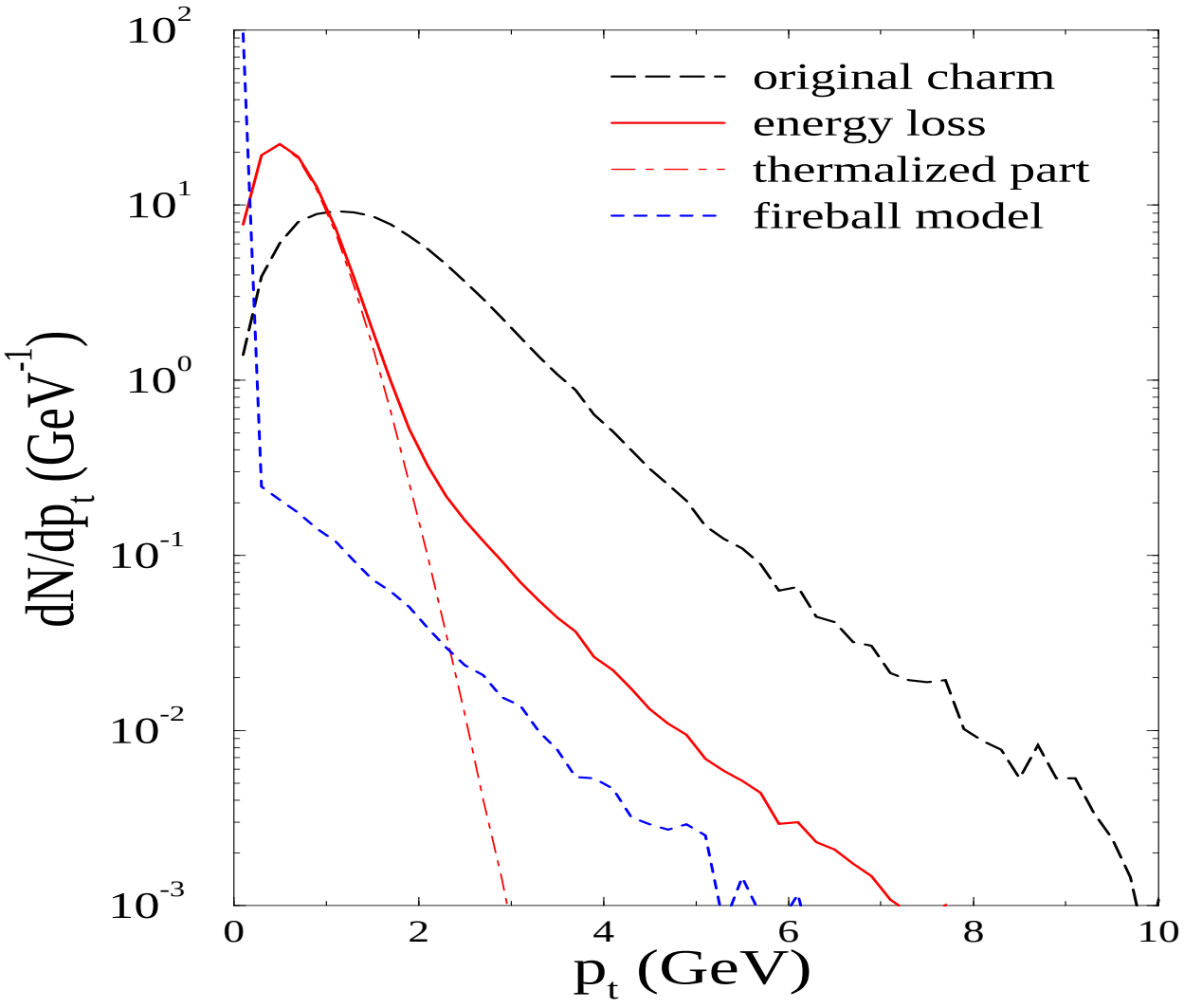

FIG. 1. The $p_\perp$ spectrum of charm and anti-charm quarks in a central Au+Au collision at $\sqrt{s} = 200$ GeV. The long-dashed curve represents the initial production without energy loss. The solid curve is our result with the energy loss ($dE/dx = -2$ GeV/fm) and the dot-dashed curve represents the part from thermalized charm quarks. The short-dashed curve is calculated with the static fireball model.

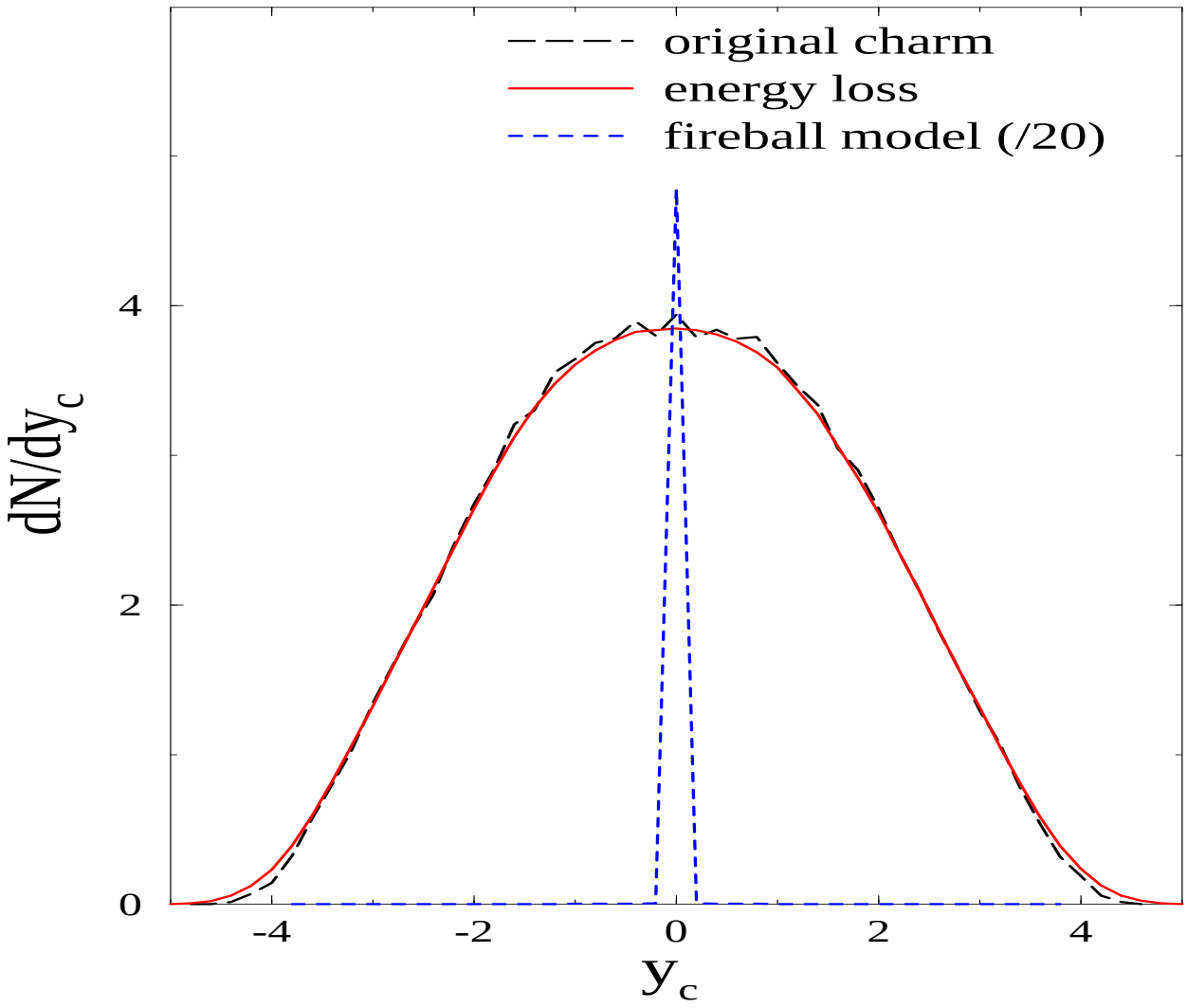

FIG. 2. Rapidity spectrum of charm and anti-charm quarks. The short-dashed curve, calculated with the static fireball model, is scaled down by a factor of 20.

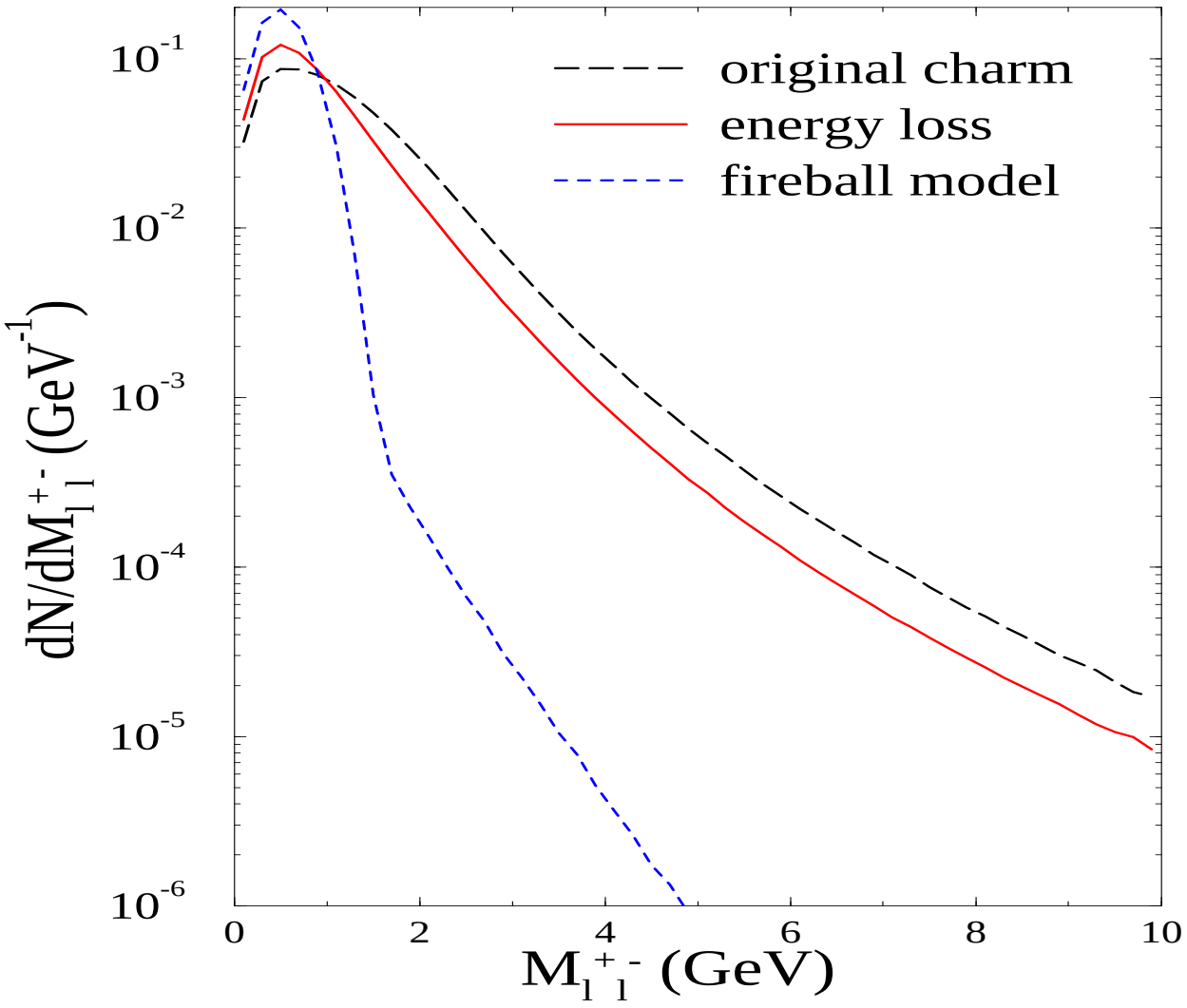

FIG. 3. Invariant mass spectrum of dileptons from correlated charm pair decays.

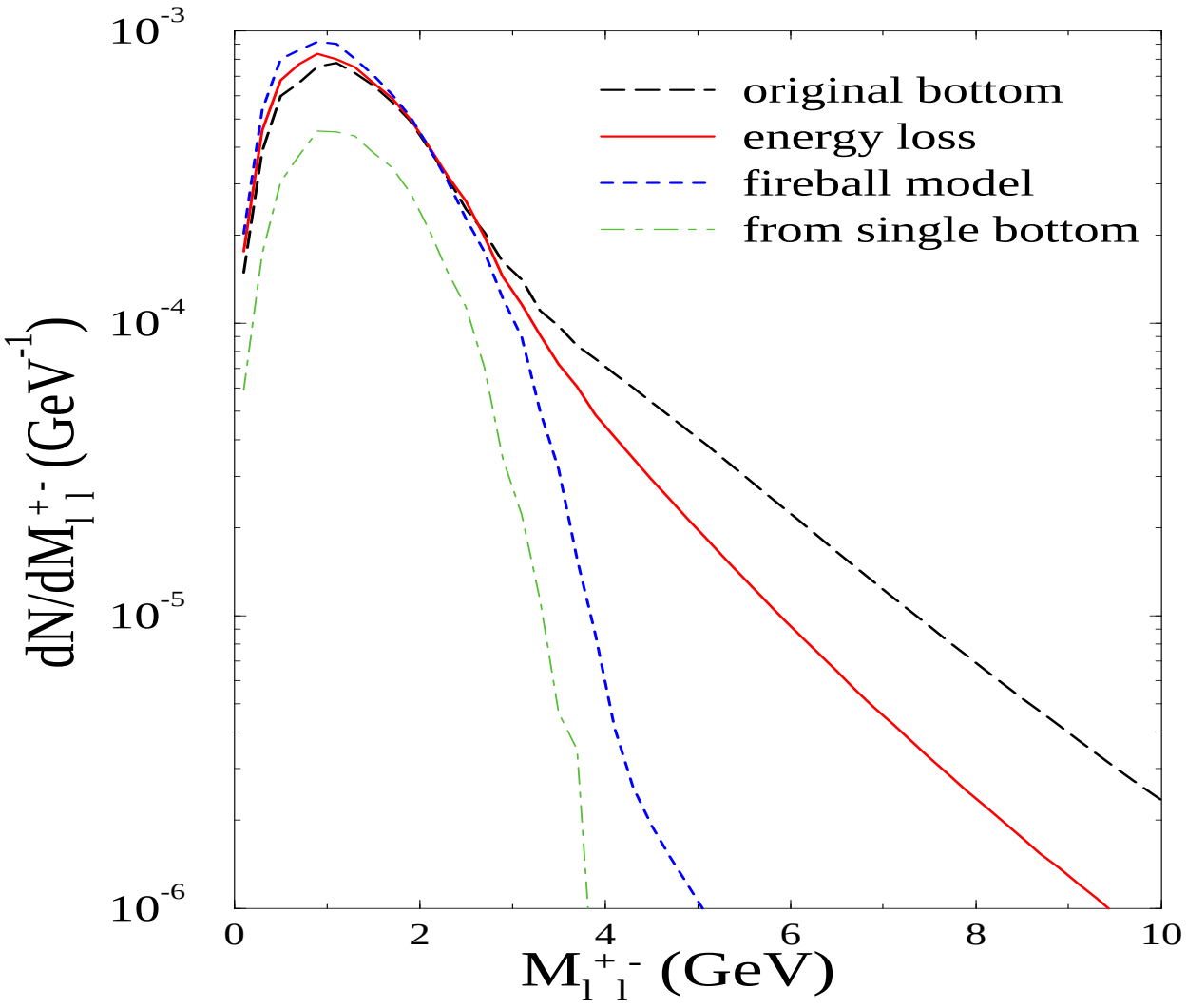

FIG. 4. Invariant mass spectrum of dileptons from bottom decays. The dot-dashed curve is the contribution from the decay of single b and $\bar{b}$ quarks.

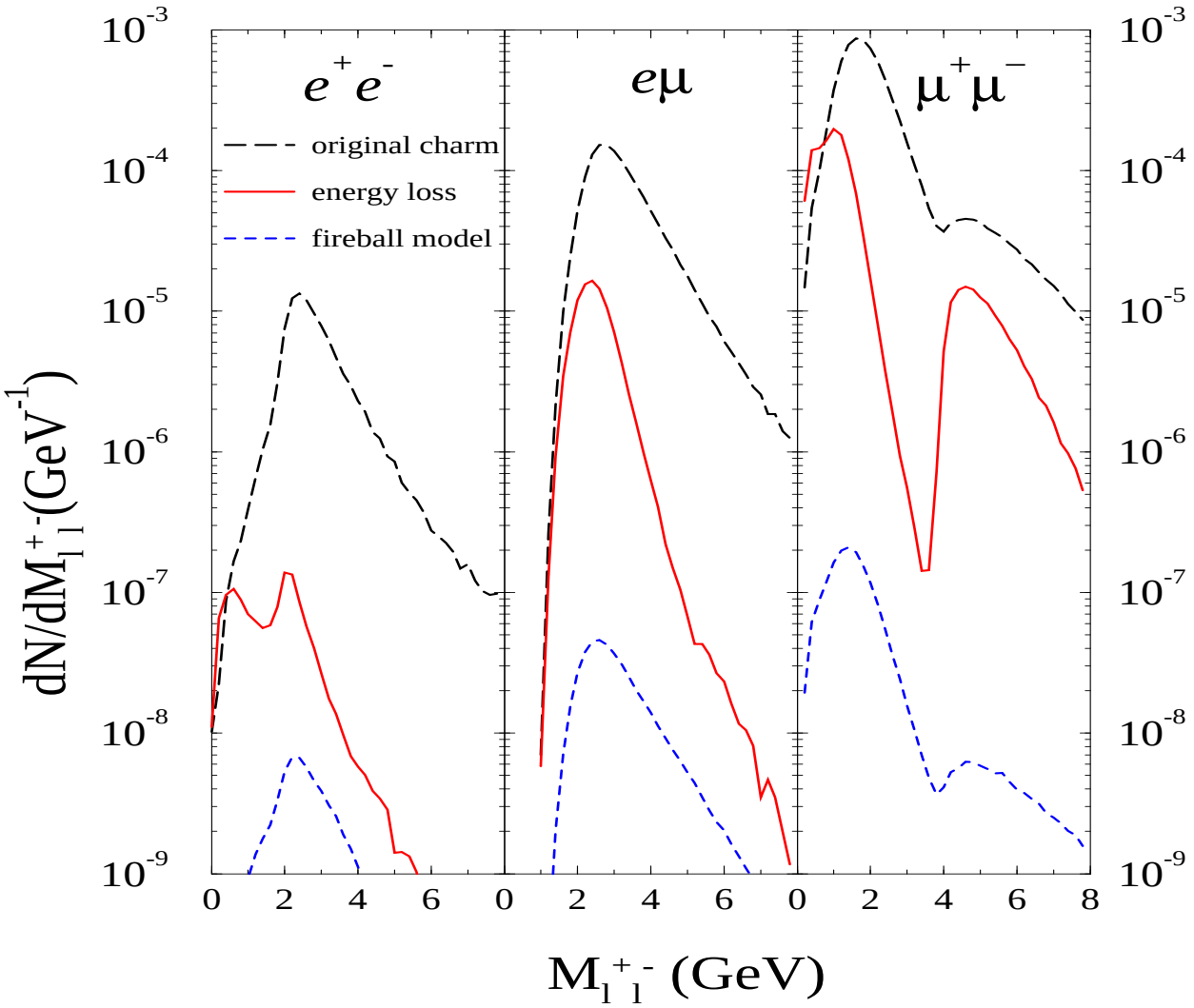

FIG. 5. Invariant mass spectra of the three dilepton channels, $ee, e\mu$, and $\mu\mu$, from correlated charm pair decays within the PHENIX acceptance.

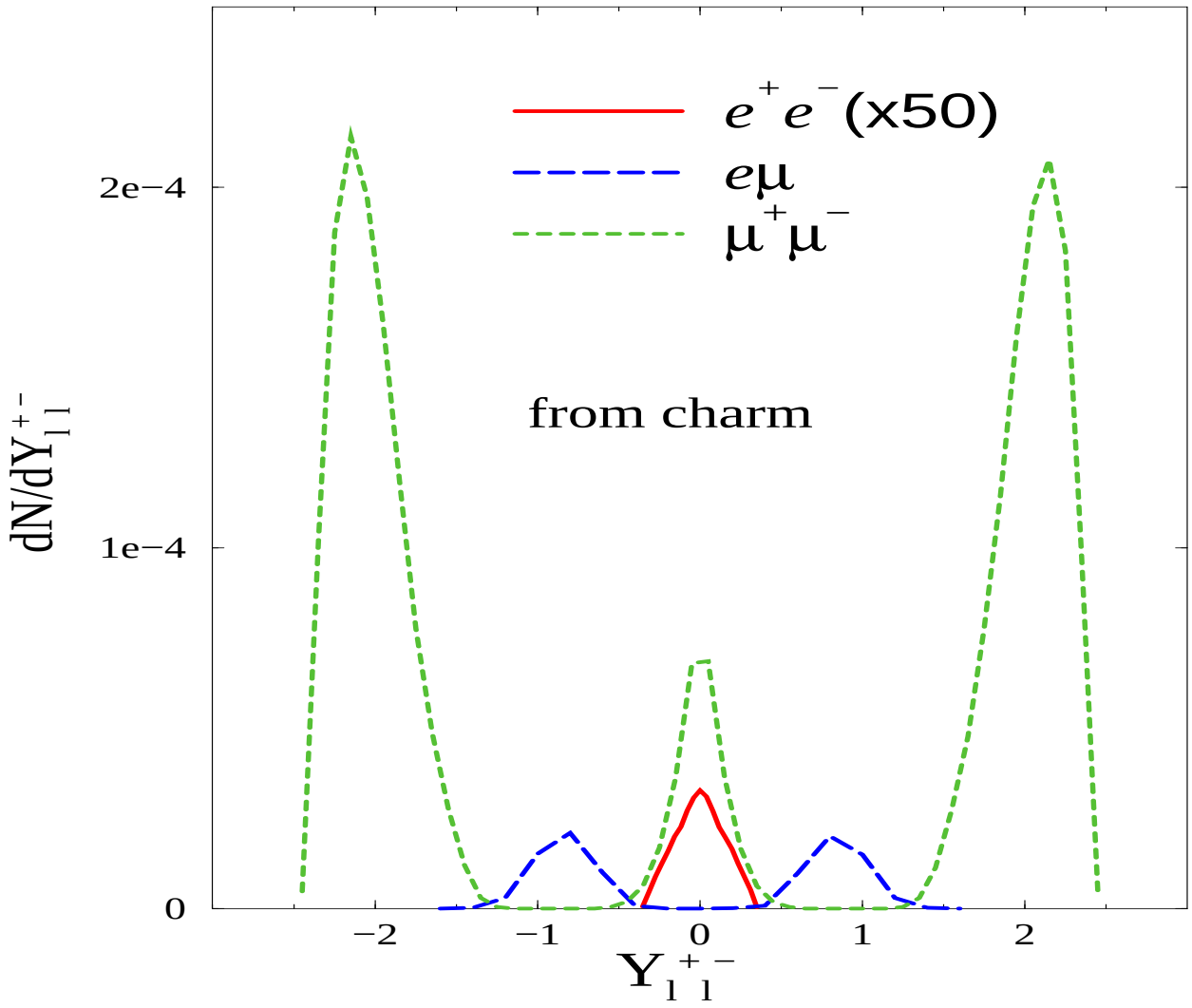

FIG. 6. Rapidity spectra of the three dilepton channels, $ee, e\mu$, and $\mu\mu$, from correlated charm pair decays within the PHENIX acceptance. The solid curve representing dielectrons is scaled up by a factor of 50. The long-dashed curve represents opposite-sign $e\mu$ pairs.

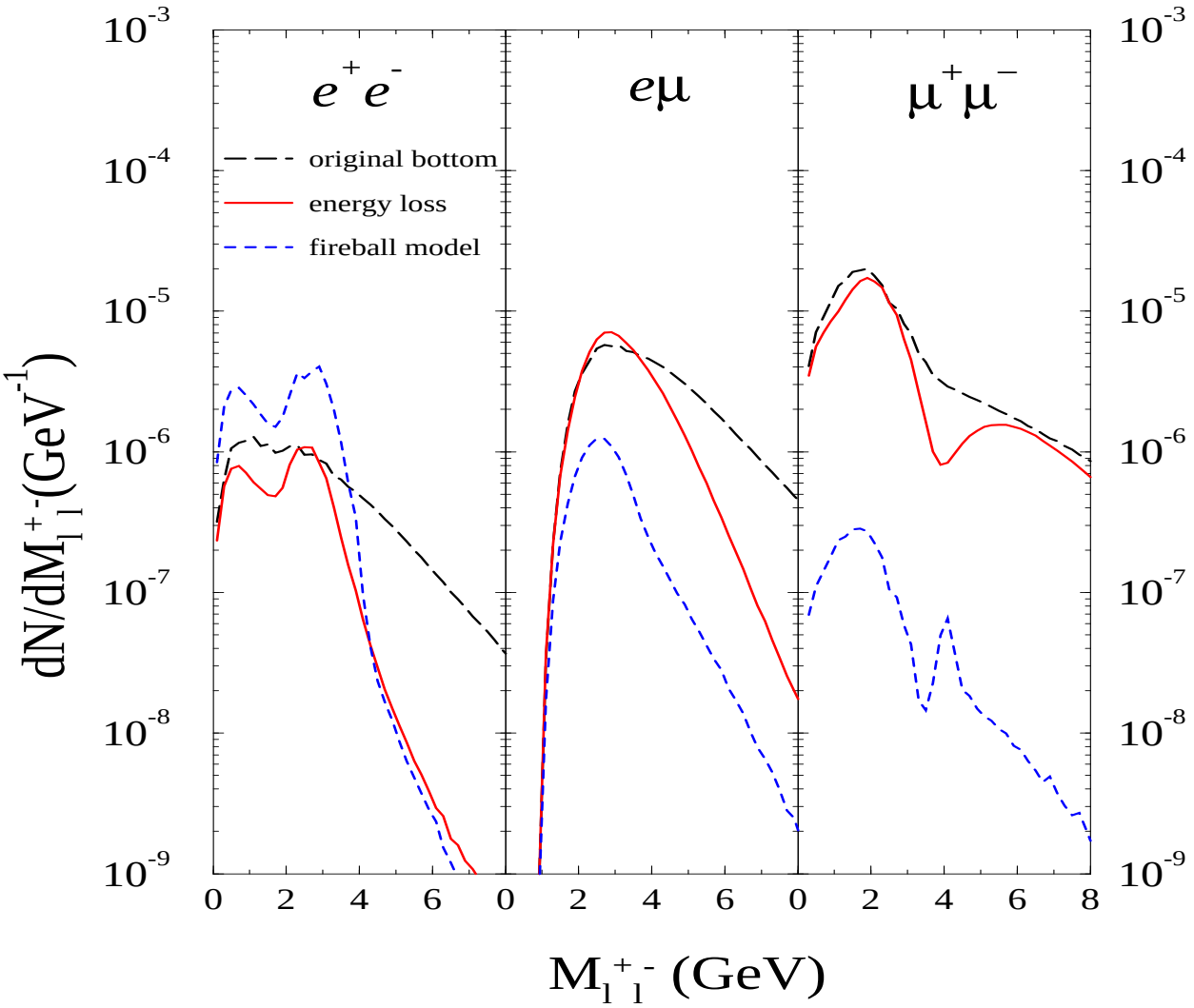

FIG. 7. Invariant mass spectra of the three dilepton channels, $ee, e\mu$, and $\mu\mu$, from bottom decays within the PHENIX acceptance.

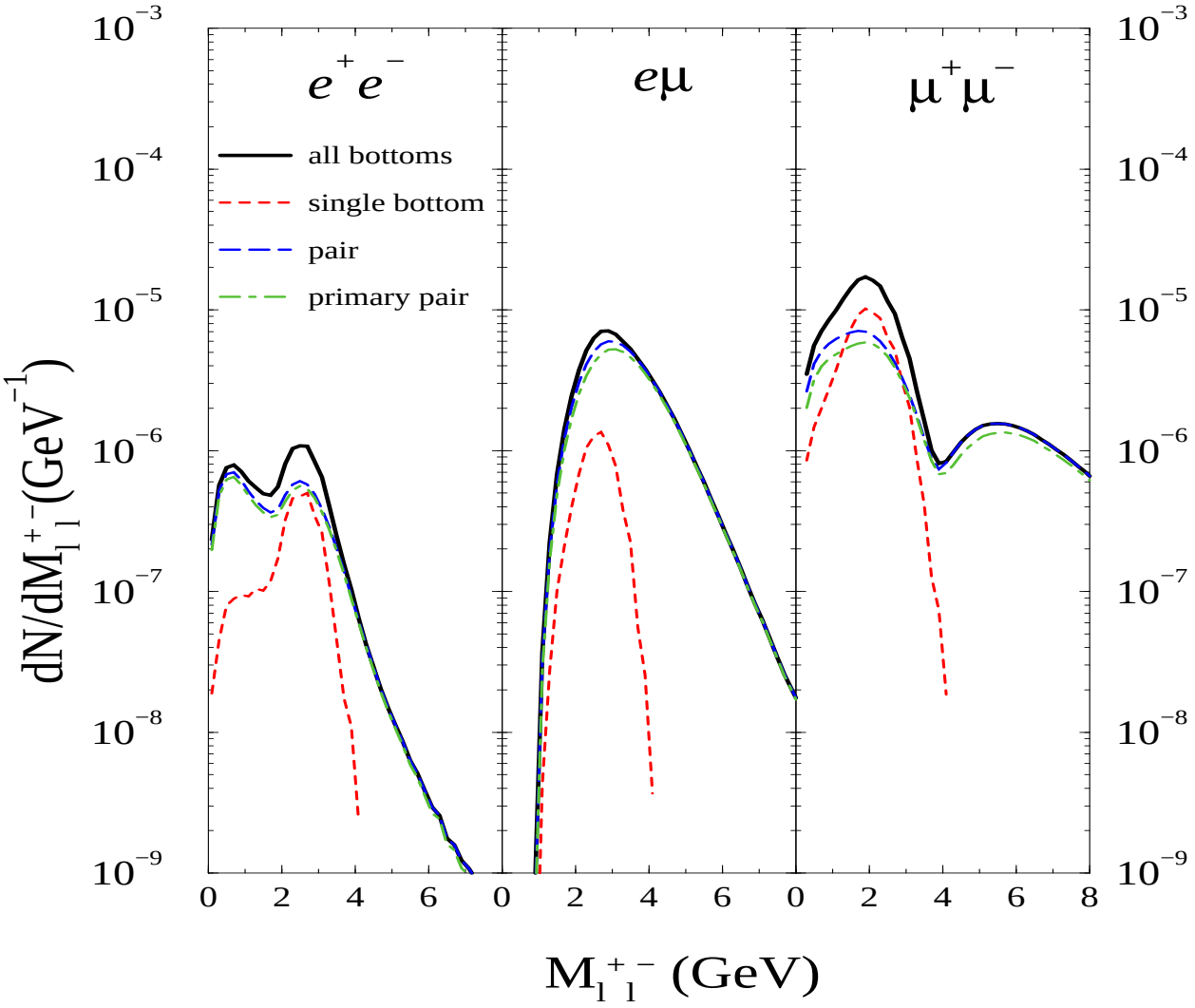

FIG. 8. The three dilepton channels from bottom decays in our model within the PHENIX acceptance. The short-dashed curves and the long-dashed curves represent dileptons from single quark decays and bottom pair decays, respectively. The solid curves represent the sum of these two curves. The dot-dashed curves represent dileptons from bottom pair decays where both leptons are primary leptons.

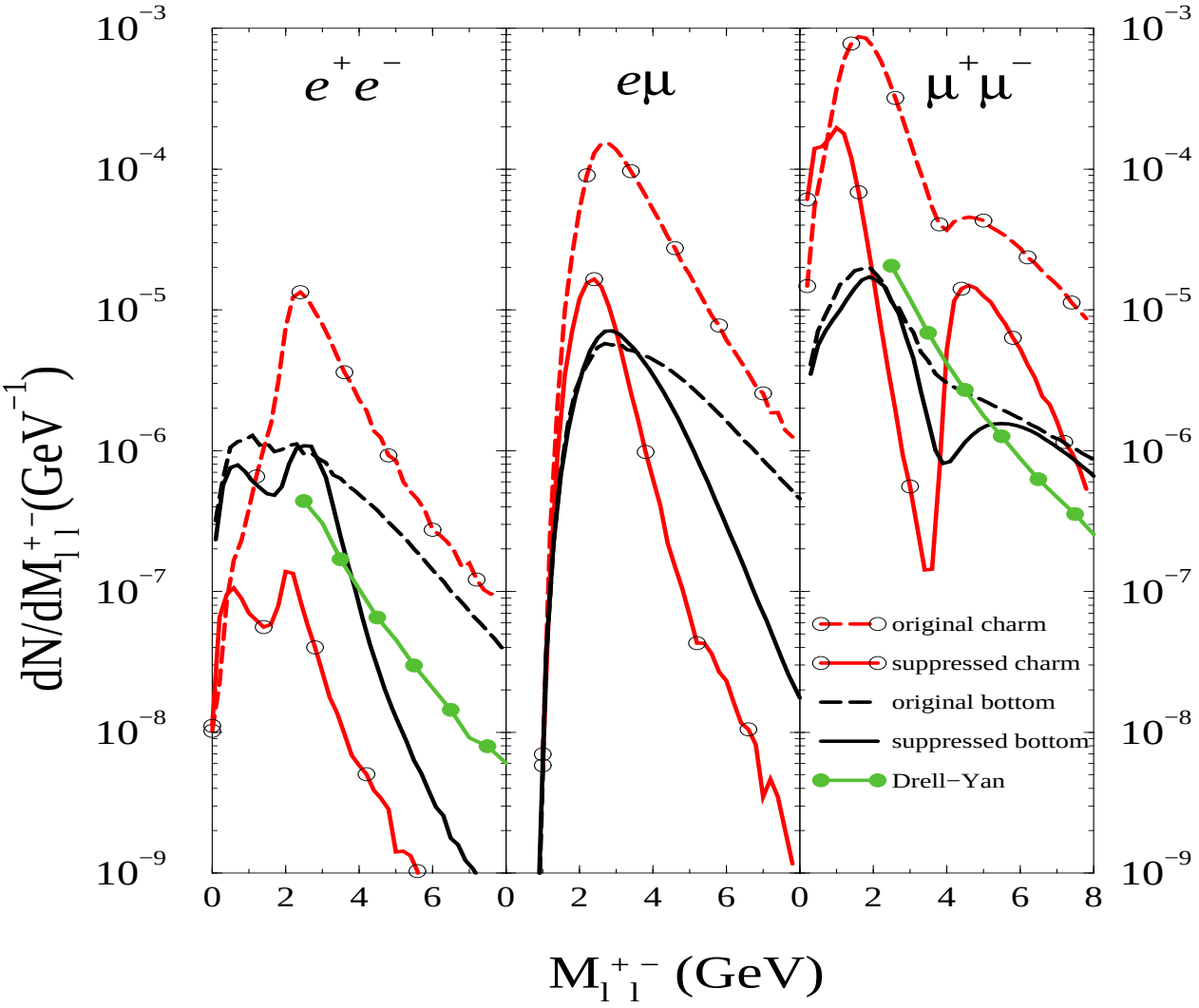

FIG. 9. Invariant mass spectra of the three dilepton channels from correlated bottom and charm decays within the PHENIX acceptance. The ee and $\mu\mu$ channels are compared to the Drell-Yan yields.

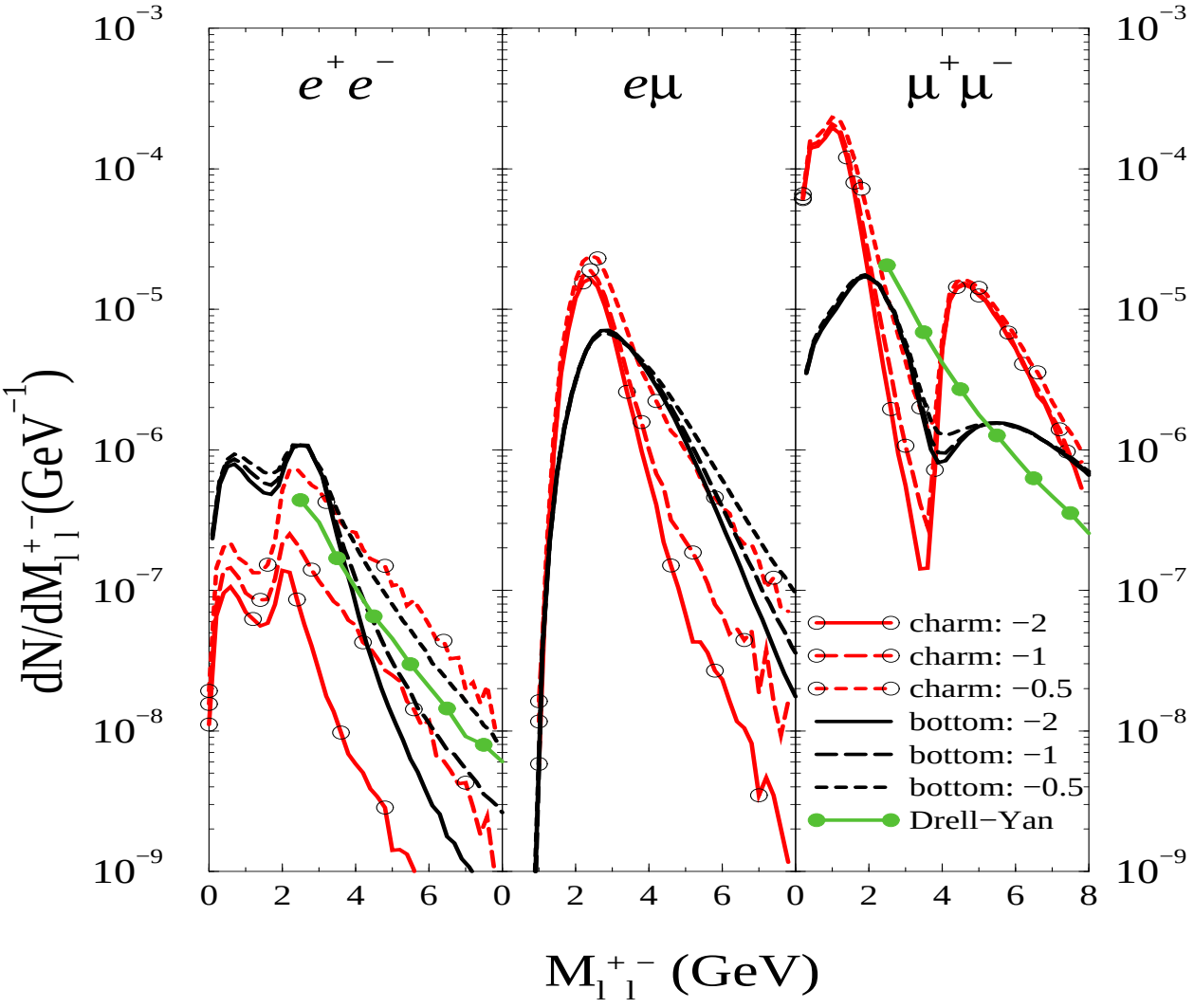

FIG. 10. Dileptons from charm and bottom decays within the PHENIX acceptance with different values of dE/dx (-2, -1, and -0.5 GeV/fm).

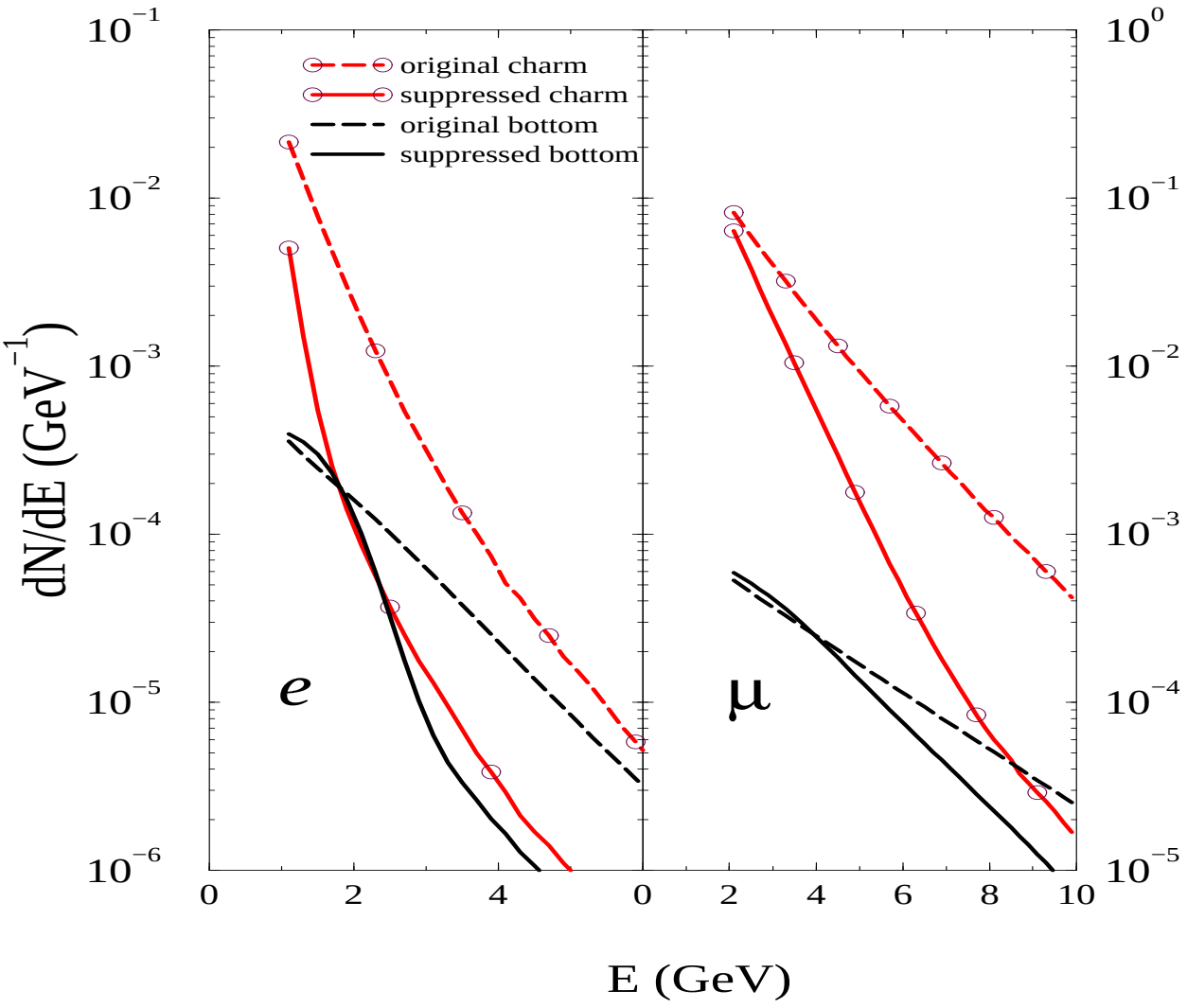

FIG. 11. Energy spectrum of single electrons and muons from charm and bottom decays within the PHENIX acceptance.

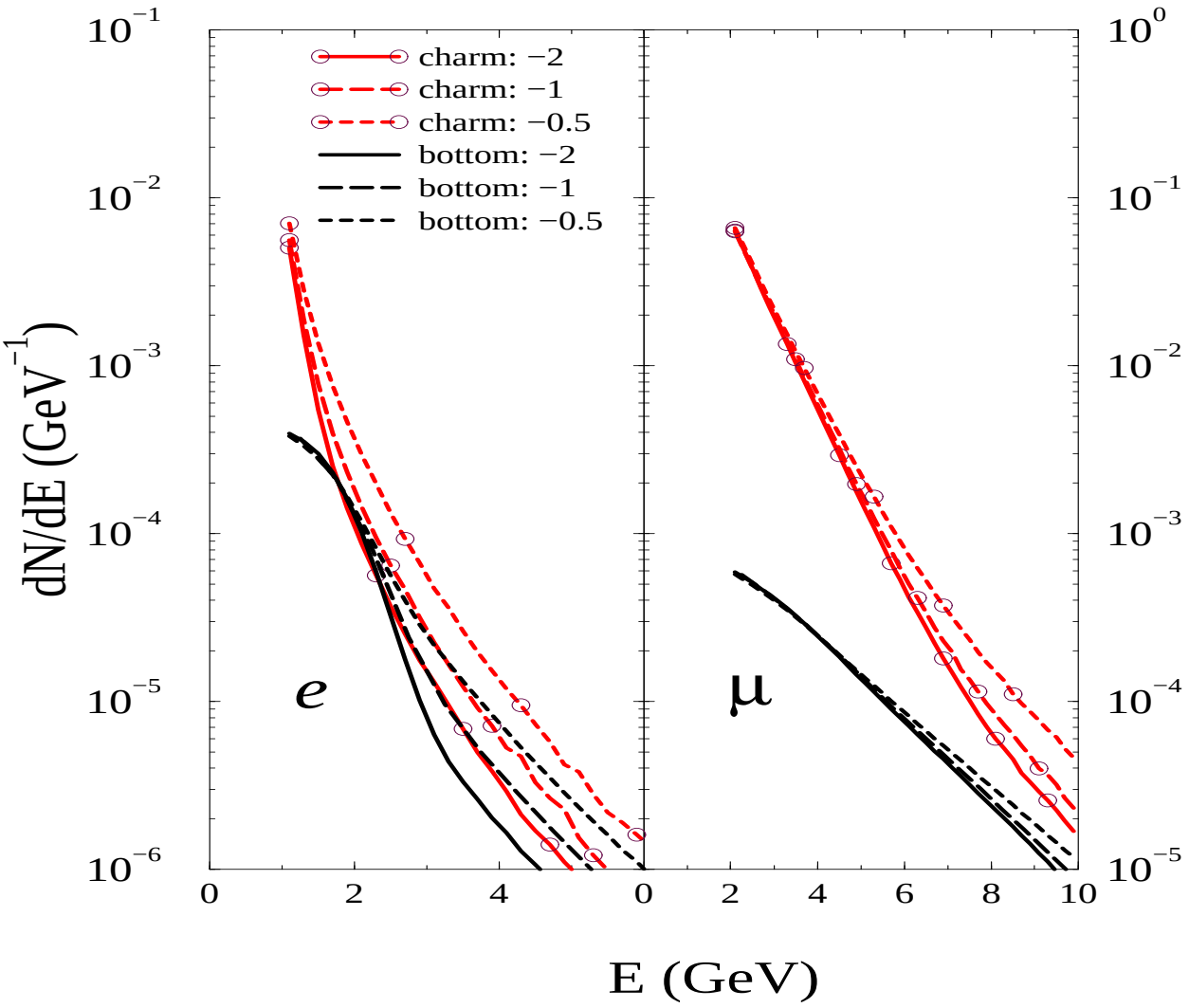

FIG. 12. Single electrons and muons from charm and bottom decays within the PHENIX acceptance with different values of dE/dx (-2, -1, and -0.5 GeV/fm).

REFERENCES

[1] M. Gyulassy and X.-N. Wang, Nucl. Phys. B420, 583 (1994); X.-N. Wang, M. Gyulassy and M. Plumer, Phys. Rev. D51, 3436 (1995).

[2] R. Baier, Yu.L. Dokshitser, S. Peigne and D. Schiff, Phys. Lett. B345, 277 (1995).

[3] R. Baier, Yu.L. Dokshitser, A.H. Mueller, S. Peigne and D. Schiff, Nucl. Phys. B478, 577 (1996); B483, 291 (1997); B484, 265 (1997).

[4] X.-N. Wang and M. Gyulassy, Phys. Rev. Lett. 68, 1480 (1992).

[5] E. Braaten and M. Thoma, Phys. Rev. D44, R2625 (1991).

[6] M. Thoma and M. Gyulassy, Nucl. Phys. B351, 491 (1991); Nucl. Phys. A544, 573c (1992).

[7] X.-N. Wang, Z. Huang and I. Sarcevic, Phys. Rev. Lett. 77, 231 (1996); X.-N. Wang and Z. Huang, Phys. Rev. C55, 3047 (1997).

[8] R. Vogt, B.V. Jacak, P.L. McGaughey and P.V. Ruuskanen, Phys. Rev. D49, 3345 (1994).

[9] S. Gavin, P.L. McGaughey, P.V. Ruuskanen and R. Vogt, Phys. Rev. C54, 2606 (1996).

[10] D. Fein, Z. Huang, P. Valerio and I. Sarcevic, Phys. Rev. C56, 1637 (1997).

[11] E. Shuryak, Phys. Rev. C55, 961 (1997).

[12] J.D. Bjorken, Phys. Rev. D27, 140 (1983).

[13] X.-N. Wang and M. Gyulassy, Phys. Rev. D44, 3501 (1991); D45, 844 (1992).

[14] P. Nason, S. Dawson and R. K. Ellis, Nucl. Phys. B303, 607 (1988); Nucl. Phys. B327, 49 (1989);

W. Beenakker, H. Kuijf, W. L. van Neerven and J. Smith, Phys. Rev. D40, 54 (1989);

W. Beenakker, W. L. van Neerven, R. Meng, G. Schuler and J. Smith, Nucl. Phys.

B351, 507 (1991).

[15] R. Vogt, Z. Phys. C71, 475 (1996).

[16] I. Sarcevic and P. Valerio, Phys. Lett. B338, 426 (1994).

[17] M.L. Mangano, P. Nason, and G. Ridolfi, Nucl. Phys. B373, 295 (1992).

[18] A.D. Martin, W.J. Stirling and R.G. Roberts, Phys. Lett. B306, 145 (1993); ERRATUM-ibid. B309, 492 (1993).

[19] R. Vogt, S. J. Brodsky and P. Hoyer, Nucl. Phys. B383, 643 (1992).

[20] E769 Collab., G.A. Alves *et al.*, Phys. Rev. Lett. 77, 2392 (1996).

[21] E.V. Shuryak, Phys. Lett. B78, 150 (1978); Sov. J. Nucl. Phys. 28, 408 (1978).

[22] T. Sjostrand, Report No. LU-TP-95-20, preprint hep-ph/9508391.

[23] MARK-III Collab., R.M. Baltrusaitis *et al.*, Phys. Rev. Lett. 54, 1976 (1985); ERRATUM-ibid. 55, 638 (1985).

[24] S. Nagamiya *et al.*, in PHENIX Conceptual Design Report (1993) (unpublished); on internet see *http://rsgi01.rhic.bnl.gov/∼ phenix/phenix_home.html*.

[25] CLEO Collab., S. Behrends *et al.*, Phys. Rev. Lett. 59, 407 (1987); B. Barish *et al.*, 76, 1570 (1996).

[26] M. Tannenbaum, Heavy Ion Phys. 4, 139 (1996).